

EXPERIMENTAL STUDY OF CONDENSATIONAL GROWTH ACTIVATION FOR CARBONACEOUS PARTICLES REMOVAL FROM FLUE GASES

G. Cozzolino*, M. de Joannon, P. Sabia**, R. Ragucci**,
A. Cavaliere***

g.cozzolino@unina.it

* Dipartimento di Ingegneria Chimica, Università degli Studi di Napoli Federico II, Naples, Italy

** Istituto di Ricerche sulla Combustione – C.N.R., Naples, Italy

Abstract

A novel technique for both industrial and domestic applications for submicronic particles removal from flue gases relies on increasing the diameter of fine and ultra-fine particles by condensing water vapor onto the particles themselves.

This study experimentally evaluated the condensational growth activation via the heterogeneous nucleation of water vapor on particles for different temperature and vapor concentration as well as the characteristic time of the condensation process.

It has been shown that it is possible to capture the dispersed particles in the water droplets with high efficiency in dependence on operative conditions. Higher inlet vapor concentration as well as lower working temperature increase the final size of the particles thus improving their removal from the gas stream. Furthermore the characteristic induction and growth times are experimentally evaluated. They are compatible with practical applications and their identification and the estimation can be very useful in the design and dimensioning of a real abatement unit.

Introduction

The presence of submicronic particles in flue gases coming from different typology of industrial plants represents a strong concern due to their well known dangerous effects on human health and environment. In the field of particle abatement one of main issues to which the research has to face with is the inefficacy of traditional physical separation processes, based on diffusion, inertial impact, as well as sedimentation, in removing particle diameters ranging from 0.1 μm to 1 μm . For this range of particle diameter the removal efficiency of traditional abatement systems decrease to approximately 25%, thereby rendering their application impractical [1]. Improvements in the operation at optimal working conditions might be facilitated by increasing the dimension of the particles to be eliminated upstream of the standard cleaning processes. A novel technique for both industrial and domestic applications relies on increasing the diameter of fine and ultra-fine particles by condensing water vapor onto the particles themselves. The easy

availability of vapor at relatively low temperatures makes this technique interesting for a wide range of industries, including chemical, glass, cement and metallurgy production systems and combustion facilities, all of which are interested in the removal of fine particles from waste gases [2]. In the field of combustion process, this technique might be even more relevant for flue gases coming from MILD (Moderate or Intense Low-oxygen Dilution) [3] or coal Oxy-Fuel Combustion processes [4], where water vapor could be used as a diluent to reduce the maximum temperature reached during combustion, thereby leading to a decrease in pollutant formation. Additionally, a high content of vapor can be present in the flue gases of biomass fuels, depending on the type of combustion facility and the feedstock characteristics. The characteristic rate of vapor nucleation on a particle is a complex function of both the ambient conditions and the particle characteristics, including morphology, dimension, charge and history. This study experimentally evaluated the condensational growth activation via the heterogeneous nucleation of water vapor on particles for different temperature and vapor concentration as well as the characteristic time of the condensation process.

Experimental configuration

A 10 cm square cross section laminar flow chamber was used for the experimental tests. The general scheme of the experimental set-up has been reported in Figure 1. A 10 cm square cross section laminar flow chamber has been used for the experimental tests. A carrier gas, steam and/or particles from a spark generator system (PALAS GFG1000) are axially fed to the chamber with a 2 cm injection tube. An inert gas flow, is fed externally to the mainstream to prevent the diffusion of the droplets and particles toward the chamber walls and at the same time for a controlled cooling of the mainstream. The steam is fed by means of an evaporator able to provide a controlled steam flow (Bronkhost C.E.M.). A remotely controlled heater system avoids the steam condensation along the feed line. A J-type thermocouple placed in proximity of the outflow section of the mainstream allows to control the temperature of the working fluid. The evolution of the condensation process has been followed along the chamber axis (z) by collecting the polarized components of laser light elastically scattered at 90° by the control volume and by computing the polarization ratio. More specifically, the second harmonic ($\lambda=532$ nm) of aNd-YAG laser has been used as excitation wavelength. The elastically scattered light is focused by a biconvex lens with a focal length $f=100$ mm on a APD type photodiode with a 1:1 magnification ratio. The dimensions both of laser beam and of detector, along with the magnification ratio of the collection system used, result in a control volume 0.5 mm tall and 3 mm deep. Polarization rotators and analyzers are placed on the optical path of the system allowing the measurements of the vertical (I_{VV}) and horizontal (I_{HH}) components of the scattered light. The collected signals along axis chamber and the intensity of incident laser beam for each pulse, are recorded by an oscilloscope and stored on a PC. Each experimental values reported represents an average value obtained from an ensemble of 2000 runs properly post-processed taking into account

background and laser intensity signals. From the averaged polarized components the polarization ratio is computed as $\gamma = I_{HH} / I_{VV}$. The choice of 90° collecting angle has been made in order both to maximize the spatial resolution and to minimize interference due to stray light. In addition, the dependence on the scatterers size of the polarized components (and hence of their polarization ratio) at a scattering angle of 90° is maximized and allows for a better discrimination between the particulate and the nucleated droplets. The polarization ratio has been measured as a function of axial coordinate. In the followings the results will be presented as a function of the residence time, t , being the axial flow velocity v constant and equal to 0.4m/s in all the conditions reported. Accordingly, a residence time t_{res} equal for all the test cases to z_{max}/v , can be defined. Temporal profiles of γ have been obtained for four vapor inlet concentration X_v (0, 0.10, 0.25 and 0.35). Thus, $X_v = 0$ corresponds to the case where only graphite particles and carrier are fed to the flow chamber. By increasing the vapor concentration from 0 to 0.35, the percentage of the carrier gas has been changed in such way that the fluid-dynamic conditions are equivalent in all the condition considered. For each vapor concentration three inlet temperatures ($T_{\text{in}} = 375\text{K}$, 405K , 425K) have been considered at a fixed confinement temperature T_c of 298K . The polarization ratio of propane has been measured with the same experimental set up as reference value for pointing out the limit of the detection system. The value of the error has been verified, according to this considerations, below 10% in all the cases here presented and below 8% for distances from the chamber inlet greater than 20 mm. The aerosol generator was operated with graphite electrodes with a spark discharge frequency of 30Hz and a carrier feed of Ar of 3.5l/min . In this condition a monodispersed particle distribution with the maximum at $D_p = 150\text{nm}$ have been measured after sampling with a Z-Sizer Nano (Malvern). This diameter corresponds to a particle number density of $4.3 \cdot 10^7$ particle/cm³.

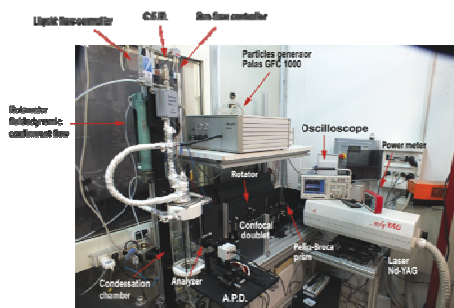


Figure 1. Experimental setup.

Results and discussion

Temporal profiles of γ were obtained for four vapor inlet concentrations, X_v (0, 0.10, 0.25 and 0.35). When $X_v = 0$, only graphite particles and carrier are fed to the flow chamber. By increasing the vapor concentration from 0 to 0.35, the percentage of the carrier gas was changed in such a way that the fluid-dynamic

conditions are equivalent for all conditions studied. For each vapor concentration, three inlet temperatures ($T_{in}=375\text{K}$, 405K , 425K) were examined at a fixed confinement temperature, T_c , of 298K . The polarization ratio of propane was measured with the same experimental apparatus as a reference value to determine the limits of the detection system. Figure 2(a) shows the value of γ evaluated at $T_{in}=375\text{K}$ for the four values of X_v . For $X_v=0$, the value of γ is almost constant with a residence time of approximately 0.1, consistent with the particle size of the feed stream. This trend suggests that coagulation occurring among the graphite particles is negligible. Although the theoretical value of the polarization ratio should be equal to zero for particle light scattering described by the Rayleigh model, the experimental literature values of the ratio collected at 90° range between 0.01 and 0.1 [5], due to the finite collecting angle of the diagnostic system. The γ values reported in Figure 3 are consistent with the calculated values after accounting for the collection system characteristics and the generated particle properties and size distributions. The condensation process was clearly present, as suggested by the profile of the polarization ratio measured in the presence of vapor. For $X_v=0.35$, and for t higher than 0.06 s, the polarization ratio sharply increased and reached a value of approximately 0.38 at $t=0.11$ s, suggesting that the scatterer diameters significantly increased. This behavior indicates that the nucleation process was suddenly activated, and the surface growth and particle coalescence lead to the formation of larger droplets.

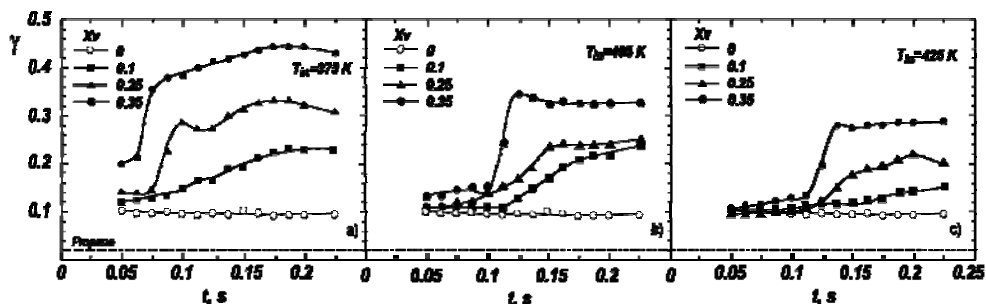


Figure 2. Polarization ratio as a function of residence time.

For $X_v=0.25$, the profiles shown in Figure 2a suggest that, while heterogeneous nucleation occurred, the increase in droplet size was limited compared with higher vapor concentrations. Different considerations apply to data collected at $X_v=0.1$. At these conditions, γ monotonically increased, reaching a plateau of 0.24 at $t=0.18$ s. The absence of a sudden increase in signal and the presence of a plateau suggest that the nucleation and growth processes are slow, leading the system to an equilibrium condition where no further change in droplet diameter can occur.

An increase in the inlet temperature delayed the collection mechanism, as seen from profiles shown in Fig. 2(b) and Fig. 2(c), where γ measured for a T_{in} of 405K and 425K are reported.

An indication of the efficiency and the characteristic time of the condensation process can be obtained by evaluating a growth factor, g_f , defined as

$$g_f = \frac{\gamma_{\text{graphite+vapor}}}{\gamma_{\text{graphite}}} \quad (3)$$

The growth factor is an increasing function of scatterer diameters and is equal to unity when no condensation occurs. In Figure 3(a) the maximum values of g_f evaluated at different X_v have been reported as a function of T_{in}/T_{sat} , where T_{sat} is the saturation temperature corresponding to the X_v considered. The growth factor increases for all values of the vapor concentration considered as soon as the system moves towards saturation conditions ($T_{in}/T_{sat} > 1$). At the lowest X_v of 0.1 the growth factor does not strongly depend on inlet temperature. It increases from 1.2 to 2.01 passing from $T_{in}/T_{sat} = 1.38$ to 1.27, then it is nearly constant up to $T_{in}/T_{sat} = 1.18$. This trend shows that for such a vapor concentration no further droplet increase can occur but an equilibrium condition between the droplet and the environment is reached. The equilibrium conditions are not reached for higher vapor concentrations where a significant increment of g_f occurs. At $X_v = 0.25$ g_f increases from 2 to 3.2 with a decrease of T_{in}/T_{sat} from 1.6 to 1.09. At $X_v = 0.35$ the growth factor reaches the value of 4.2. It is noteworthy to underline that in the range of T_{in}/T_{sat} between 1.3 and 1.18 the growth factor has a nearly equal value for all the conditions considered, that varies from 2 to 2.3. In addition, the dependence on T_{in}/T_{sat} of droplet condensation and their growth appears very similar when the system is far from the equilibrium conditions, independently of the T_{in}/T_{sat} range. Figure 3(b) shows the induction time, t_{ind} , of the nucleation and growth process (empty symbols) that corresponds to the time of the first sudden increase in the polarization ratio. The same diagram shows the time t_{max} , the time that the particle reaches its maximum size (full symbols) and g_f reaches a maximum. For vapor concentrations equal to 0.35 and 0.25, it is possible to distinguish the t_{ind} from t_{max} . At $X_v = 0.1$, the system slowly changed toward the final droplet dimension such that only t_{max} can be reported. As seen in the figure, the higher the X_v , the lower the induction time. Additionally, t_{ind} was very sensitive to T_{in} . The same considerations applied for t_{max} , even though the dependence on T_{in} was smoother.

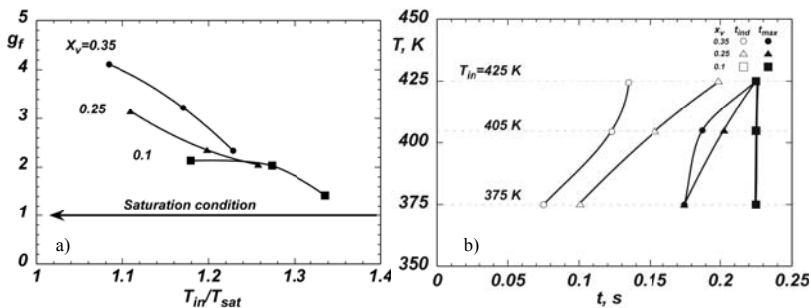


Figure 3.(a) Growth factors and (b) characteristic times of the process as a function of time for different operating conditions.

Conclusions

An evaluation of the particle abatement by means of condensational growth demonstrated that the dispersed particles, acting as condensation nuclei, were captured in the nucleated water droplets with high efficiency, depending on the operating conditions. As expected, the higher the vapor concentration as well as the lower the working temperature, the higher the final size of the particles. Thus, for $X_v=0.35$ the growth factor increases from 2.3 up to 4.2 for T_{in} changing from 425K to 375K. It is worth noting that also potentially extreme working conditions can be very useful for the particle covering. In fact, the nucleation and growth processes are active also at very low vapor concentration, although the maximum growth factor in this condition is relatively low. Thus, it could be of interest to split the abatement process in successive steps at different vapor concentrations, on the basis of the context of the application. After a first condensational growth unit, the decrease to zero of the contact angle due to water layer present on the particles makes the nucleation rates in a successive condensational growth unit strongly increase. In addition, the successive growths can be exploited to have a higher control of the final dimension of the droplet according to the downstream unit used for droplet removal. This twofold effect can lead to a significant increase of the overall plant efficiency. Very similar considerations apply for the dependence of the process on the inlet temperature. As final consideration, it is worth note that the characteristic induction and growth times experimentally evaluated, are compatible with practical applications. Furthermore, their identification and the estimation can be very useful in the design and dimensioning of a real abatement unit. In particular, the data presented in this work have a broad and intrinsic relevance because they have been collected in a simple system where the single subprocesses can be temporally resolved in a wide range of parameters.

Acknowledgment

This work is financially supported by Ministero dello Sviluppo Economico within the Accordo di Programma CNR-MSE, Gruppo Tematico Carbone Pulito – Fondo per il Finanziamento Attività di Ricerca e Sviluppo di Interesse Generale per il Sistema Elettrico Nazionale (http://www.ricercadisistema.cnr.it/images/det/libroMSE_2anno.pdf).

References

- [1] <http://www.epa.gov/apti/bces/module3/collect/collect.htm>
- [2] C. Ehrlich, G. Noll, W.-D. Kalkoff, G. Baumbach, A. Dreiseidler, PM₁₀, PM_{2.5} and PM_{1.0}—Emissions from industrial plants—Results from measurement programmes in Germany, *Atmospheric Environment*, 41, 29, (2007), 6236-6254
- [3] A. Cavaliere, M. de Joannon, MILD combustion, *Prog. Energy Combust.*, 30 (2004), pp. 329–366
- [4] B.J.P. Buhre, L.K. Elliott, C.D. Sheng, R.P. Gupta, T.F. Wall, Oxy-fuel combustion technology for coal-fired power generation, *Progress in Energy and Combustion Science* 31 (2005) 283–307
- [5] Beretta F., Cavaliere A., D' Alessio A., *Combust. Sci. Tech.* 36(1):19-37 (1984). vapor mixtures on insoluble and soluble particles, *Physical Review E* 67 021605 (2003).